Development and Validation of a Submodel for Thermal Exchanges in the Hydraulic Circuits of a Global Engine Model

Alberto Broatch, Pablo Olmeda, Jaime Martin and Josep Salvador-Iborra
Universitat Politècnica de València

Abstract

To face the current challenges of the automotive industry, there is a need for computational models capable to simulate the engine behavior under low-temperature and low-pressure conditions. Internal combustion engines are complex and have interconnected systems where many processes take place and influence each other. Thus, a global approach to engine simulation is suitable to study the entire engine performance. The circuits that distribute the hydraulic fluids –liquid fuels, coolants and lubricants- are critical subsystems of the engine. This work presents a 0D model which was developed and set up to make possible the simulation of hydraulic circuits in a global engine model. The model is capable of simulating flow and pressure distributions as well as heat transfer processes in a circuit. After its development, the thermo-hydraulic model was implemented in a physical based engine model called Virtual Engine Model (VEMOD), which takes into account all the relevant relations among subsystems. In the present paper, the thermo-hydraulic model is described and then it is used to simulate oil and coolant circuits of a diesel engine. The objective of the work is to validate the model under steady-state and transient operation, with focus on the thermal evolution of oil and coolant. For validation under steady-state conditions, 22 operating points were measured and simulated, some of them in cold environment. In general, good agreement was obtained between simulation and experiments. Next, the WLTP driving cycle was simulated starting from warmed-up conditions and from ambient temperature. Results were compared with the experiment, showing that modeled trends were close to those experimentally measured. Thermal evolutions of oil and coolant were predicted with mean errors between 0.7ºC and 2.1ºC. In particular, the warm-up phase was satisfactorily modeled.

Introduction

Nowadays, computational models are fundamental tools for engine design. For internal combustion engines, tools allowing to integrate the different components acquire an outstanding importance. Many complex processes take place in the engine and they significantly influence each other. Therefore, to thoroughly model engine performance under dynamic conditions a global, multi-domain approach is essential. With this in mind, a software called Virtual Engine Model (VEMOD) has been developed at CMT-Motores Térmicos [1]. This computational tool arises as a response to highly limiting requirements of emission standards imposed by new homologation procedures, closer to real-world driving conditions in terms of engine dynamic operation and ambient conditions (low temperature and altitude). Current context demands the support of new computational tools able to accurately predict engine performance and emissions while reducing the cost of expensive tests campaigns, usually based on chassis dyno calibration and road validation.

Different approaches can be used to model engine processes [2]. The fastest option in computational terms is the use of ad-hoc mathematical models based on data from measurements. It requires a substantial experimental effort and its lack of physical foundation deters extrapolations out of the tested conditions [3]. At the other end, 3D numerical models simulate physical phenomena with great accuracy and resolution at the cost of a high computational demand [4]. VEMOD combines 1D and 0D simulation to attain a compromise between accuracy and computation time. Main VEMOD submodels are physical, while some lesser submodels are based on well-stablished empirical correlations. This makes possible to trust the model results over a large operation range.

Thermal management plays an important role in engine operation. Improvements of the thermal performance of cooling and lubricating systems promise to deliver a reduction of emissions. Diverse authors have reported reductions of unburned hydrocarbons (HC) [5], nitrogen oxides [6] and carbon monoxide (CO) [7] after optimizing the cooling system. Moreover, emissions of carbon dioxide (CO_2) and fuel consumption can be cut through improved cooling and lubrication strategies: optimized cooling by controlling the coolant flow [8], lower friction losses by controlling the lubricant temperature [9] or reduced ancillary losses through electrification [10]. A critical target for thermal management is warm-up shortening, which allows the engine to reach nominal temperatures earlier. This leads to less HC and CO emissions [11], lower friction, reduced heat loss [12] and faster catalyst light-off [13]. Means of hasting warm-up are: coolant path optimization [14], exhaust heat recovery [15], immersion heaters, thermal mass reduction, thermal energy storage and improvement of heat transfer between oil and coolant [16].

In this context, modeling the hydraulic circuits of the engine (liquid fuel, coolant and lubricant) becomes necessary to assess potential improvements in thermal management. Any new model must be closely connected with the right engine components and it should be flexible enough to allow the study of diverse circuit layouts, hardware modifications, new technologies and different operation strategies. Several related works can be found in the literature. Luptowski et al. linked a cooling circuit model with GT-Power and concluded that fuel savings could be attained through controlled operation of the pump and the fan [17]. Cipollone et al. developed a flexible model of the cooling system [18] and coupled it to an engine heat transfer model to study split-cooling in the New European Driving Cycle (NEDC) [19]. Torregrosa et al. coupled an engine heat transfer model to a cooling circuit model and explored the benefits

that could be obtained in the NEDC by using a circuit layout which shortened engine warm-up [20]. Caresana et al. used simulation data, a cooling circuit model and a heat transfer model to compare different cooling systems in various driving cycles [21]. A more integrated approach was followed by Park et al. [22] and Banjac et al. [23]. Park et al. developed a model of the cooling system coupled to models of the vehicle, cylinder and radiator. They achieved a successful validation under diverse steady-state conditions. Banjac et al., simulated the engine, the vehicle and the thermal management system, similarly to the present research. However, some major differences between this work and theirs are: their gas path model was simpler, they used Wiebe laws instead of physically simulating combustion and heat rejection calculation was different. They analyzed the convenience of replacing the mechanically driven coolant pump by an electrically driven pump in two driving cycles. Fuel saving was merely around 1%, but other gains derived from the reduction of the warm-up time were reported.

This paper presents and validates a model to simulate thermo-hydraulic circuits. The model is capable of analyzing the hydraulic network to obtain flow rates and head loss distribution of the liquid. In addition, spatial distribution and temporal evolution of fluid temperature are simulated. Heat transfer in the circuit is taken into account in conformity with the models of connected elements. The thermo-hydraulic model is fully integrated in VEMOD as a submodel. Therefore, the validation procedure consisted in modeling the entire engine used for the experimental campaign, simulating the experimental tests and then comparing the simulation outputs with the experimental measurements. In this paper, the outputs of the thermo-hydraulic model were evaluated. In particular, oil and coolant circuits were modeled. The main objective of this study is to capture the evolution of oil and coolant temperature, since those temperatures are important for engine performance. In the following sections, the experimental setup and the test procedure are explained. Next, the thermo-hydraulic model and the global engine model are described. Thereafter, the results of the steady-state validation are examined. Finally, the outcomes of the transient validation are discussed. The test chosen to evaluate transient performance is the Worldwide harmonized Light vehicles Test Cycle (WLTC), which has replaced the New European Driving Cycle (NEDC) as standard emissions test in the European Union [24].

Methods

Experimental campaign

The engine used for validation is a 1.6 liter, four-stroke diesel engine compliant with Euro5 emissions regulations. The engine has four cylinders with four valves per cylinder. A variable geometry oil-cooled turbocharger is coupled to the engine. The engine allows to recirculate low pressure and high pressure exhaust gas into the cylinders. Engine thermal management is improved with an electrovalve which blocks coolant flow through the engine during warm-up. Main specifications can be found in Table 1.

The test cell is equipped with different measurement systems. Table 2 contains the relevant instruments for this study. Data was acquired at a frequency of 10 Hz by means of a test automation system.

Table 1. Engine specifications.

Displaced volume	1598 cc
Stroke	79.5 mm
Bore	80 mm
Compression ratio	15.4:1
Torque (max.)	320 Nm @ 1750 rpm
Power (max.)	96 kW @ 4000 rpm

Table 2. Test cell instrumentation.

Variable	Instrument	Range	Accuracy
Engine speed	Dynamometer	0-7500 rpm	±1 rpm
Torque	Dynamometer	0-400 Nm	±0.5%
Fluid temperature	k-type thermocouple	70-1520 K	±2 K
Coolant flow	Flowmeter	4.5-90 L/min	±0.5%
Oil pressure	Piezoresistive transducer	0-10 bar	±25 mbar

First part of the test campaign consisted of 22 operating points, which are summarized in Table 3. Combinations of engine speed and load were selected under two criteria: covering a large area of the engine map and being included in the WLTC range, or close to it. The three underlined combinations were also tested under cold ambient conditions (-7ºC). Engine operating parameters were set according to the calibration included in the engine control unit (ECU). Three repetitions of each operating point were measured.

Table 3. Test matrix. Steady-state tests.

Engine speed	Load
1000	21, 44, 66, 88
1250	13, 26, 50, 76, 100
1500	11, 25, 50, 75, 100
2500	25, 50, 75, 100
3500	25, 50, 75, 100

To evaluate the transient behavior of the model, the engine was operated to follow the Worldwide harmonized Light vehicles Test Procedure (WLTP) driving cycle. In the first transient study, the cycle was measured starting from hot conditions, i.e., oil, coolant and engine structure were already warmed up. Starting from hot conditions allowed to have the thermostat in action. In the second transient study, the cycle was measured starting from ambient temperature to examine the engine warm-up. Initial temperature was 20ºC. Again, operating parameters were determined by the ECU calibration. Three repetitions of each test were measured.

Virtual Engine Model (VEMOD)

VEMOD is an engine model which covers the calculation of several physical processes, as sketched in Figure 1. Air management is computed by means of a 1D gas dynamics model [1]. The model deals with flow properties transport along the intake and the exhaust systems as well as the high and low pressure EGR paths [25]. Specific submodels are considered for the boosting system, i.e. compressor [26] and turbine [27] models, air-charge and EGR coolers, throttle valves, heat transfer including gas-to-wall heat exchange and wall temperature prediction, etc. The gas dynamics model is coupled to a cylinder model whose main function is the prediction of in-cylinder conditions based on the combustion process

[28,29]. A detailed heat transfer model is used to obtain the heat rejection to chamber walls, coolant and oil [30]. A mechanical losses model [31] allows obtaining the brake power. An emission sub-model is coupled to the combustion process to predict raw CO, HC, NOx, and soot emissions as a function of the engine operating conditions. Different exhaust aftertreatment systems, such as DOC, DPF and deNOx systems, i.e. LNT or SCR, can be considered. Aftertreatment sub-models combine thermo-and fluid-dynamic with chemical modelling in order to assess the tailpipe emissions [32,33].

Finally, the engine model is coupled to two additional sub-models providing the capability to simulate driving cycles. On one hand, a control system model emulates the electronic control unit (ECU) of the engine. ECU sets different engine actuators, as throttle position, EGR valves, VGT, etc., according to engine sensors information. In particular, throttle demand is imposed by the driving cycle being simulated. The vehicle model manages the vehicle response, which determines the engine speed as main input for the engine model.

VEMOD uses four different time scales to simulate the different engine processes. Gas dynamics and in-cylinder thermodynamics are calculated with a time-step which varies to ensure numerical stability. Injection, combustion and emissions formation may require smaller time steps. In such case, the current time step of the gas-dynamics model is divided into smaller parts. Thermal evolution of the engine block and the liquids is solved once per cycle. Control system and vehicle model are integrated with a fixed time step of 20 ms. Many processes are executed in parallel, benefiting from multithreading.

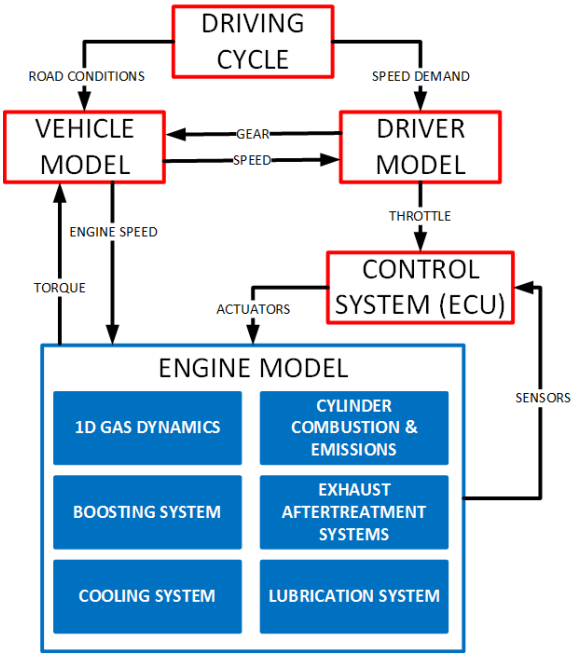

Figure 1. Flow-chart of Virtual Engine Model (VEMOD) modules.

Thermo-hydraulic model

At the beginning of the simulation, VEMOD main execution creates a separate thermo-hydraulic model for each hydraulic circuit in the engine. Circuit configuration and components can be defined in detail. Each circuit model is then called at the end of every engine cycle. The thermo-hydraulic model interacts with other models included in VEMOD. Figure 2 shows the connections of those models with the thermo-hydraulic model. Some models provide inputs to the circuit. In particular, engine speed or a reference rotational speed is multiplied by a fixed user-defined ratio to obtain pump speed. Moreover, control actuators can set the opening degree of valves. Opening degrees of thermostats depend on the temperatures in the circuit and thus are determined internally. Thermostats are modeled with a logistic curve with no hysteresis:

$$\theta = \left(1 + e^{-k(T-x_0)}\right)^{-1} \quad (1)$$

$$k = -\frac{ln(\gamma)}{T_c - x_0} \quad (2)$$

Where θ is the opening degree, which varies from 0 (fully closed) to 1 (wide open), T_c is the temperature at which the thermostat closes completely, x_0 is the mean between the T_c and the wide-opening temperature, and γ is a factor that determines the curve slope. Hysteresis can be critical when the thermostat strokes well into opening and then begins to close again. In the present study, this is not the case since the maximum opening degree of the thermostat was 35%, momentarily. The model can work using a curve with hysteresis, but defining such curve was not a pressing concern because the initial intention is to use the thermo-hydraulic model to perform warm-up simulations, during which the thermostat is closed.

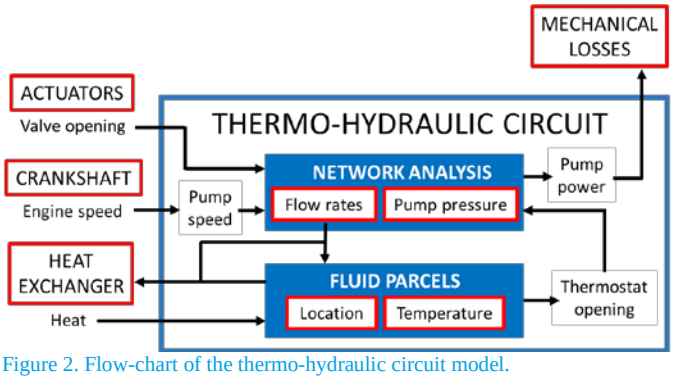

Figure 2. Flow-chart of the thermo-hydraulic circuit model.

Once the circuit configuration is determined, given a known pump speed, an analysis of the hydraulic network is performed to calculate flow rates and head losses in every element of the circuit (see next section for more details on the network analysis). Flow rate through the pump and pump pressure allow to determine power consumed by the pump with Eq. (3). This output is necessary to compute mechanical losses in the engine. In Eq. (3), η is efficiency given by a user-defined curve in terms of the pressure and flow rate. Pump pressure is calculated from the head increment in the pump, according to Eq. (4).

$$\dot{W} = \frac{p\,\dot{V}}{\eta(p,\dot{V})} \quad (3)$$

$$p = \rho\, g\, \Delta H_{pump} \quad (4)$$

The second part of the thermo-hydraulic model deals with the parcels of fluid. To model the temperature distribution throughout the circuit, the flowing fluid is divided into parcels. Each fluid parcel has a different temperature. Parcels are displaced and distributed among branches according to the flow rates calculated in the previous step. Temperature of the parcels is updated taking into account the heat provided by the heat exchanger models. In VEMOD, some heat exchangers are modeled with the NTU method according to the heat exchanger type [34]. Nevertheless, in complex elements such as the

engine block or the turbocharger, heat rejection is obtained with detailed lumped thermal networks. In the *Heat exchange* section, more details about the heat transfer process can be found. Heat exchanger models receive two variables from the circuit: flow rate through the exchanger and fluid temperature at the inlet. All heat transfer is assumed to take place in heat exchangers. Pipes and junctions are considered adiabatic.

Hydraulic network analysis

Resolution of the hydraulic network to calculate flow rates and pump head is accomplished applying Kirchhoff's laws under quasi-steady-state assumption [35]. First law states that the algebraic sum of all flow rates meeting at a junction is zero, in order to comply with mass conservation, Eq. (5). Second law is based on energy conservation. It states that, for a particular direction around a closed loop (mesh), the sum of head differences is zero. This is expressed by Eq. (6), where the sign of head differences depends on the chosen direction of the loop. Head differences are calculated with a resistance coefficient R which can multiply flow rate or, more commonly, flow rate squared. In the particular case of pipes, hydraulic resistance is calculated with Darcy-Weisbach equation. Those laws generate the system of equations shown in Eq. (7). Vector X contains the unknowns to be calculated (flow rates and, in the case of volumetric pumps, pump heads), R_i are hydraulic resistance coefficients that multiply the unknowns and C is a vector of known values.

$$\sum \dot{V} = 0 \tag{5}$$

$$\sum \Delta H = 0 \rightarrow \sum R_2 \dot{V}^2 + \sum R_1 \dot{V} + \sum R_0 = 0 \tag{6}$$

$$[\, R_2 \,][\, X\,|X|\,] + [\, R_1 \,][\, X \,] + [\, R_0 \,]\left[\frac{X}{|X|}\right] + [\, C \,] = 0 \tag{7}$$

To solve the system of nonlinear equations, an algebra C++ library called *Eigen* was used [36]. Powell's conjugate direction method was employed [37]. Junctions were assumed ideal, so they did not produce head losses.

Heat exchange

Heat transfer takes place between heat exchanger elements and fluid parcels. Heat exchangers of the present study are the following: engine cylinders, turbocharger, oil cooler, low-pressure EGR cooler, high-pressure EGR cooler and a water-cooled heat exchanger to control coolant temperature. They can be found in Figure 3 and Figure 4, which show the layouts of the oil and cooling circuits, respectively.

Heat exchangers calculate heat and store a cycle-integrated value. Once per engine cycle, the thermo-hydraulic model receives the value of heat rejected or absorbed by every heat exchanger. Next, a new parcel is created with a volume equal to the volume of the heat exchanger. To determine the new parcel temperature T_0, temperature of all parcels currently inside the limits of the heat exchanger is mass averaged. Then, temperature of the new parcel is updated using the heat value, Q, and Eq. (8).

$$T = T_0 + \frac{Q}{m\, c_p(T_o)} \tag{8}$$

Fluid parcels are later displaced according to the flow rate in that branch. If flow is not zero, some volume of fluid enters the heat exchanger. It can be formed by one parcel or by more than one. In the latter case, temperature of the entering parcels is mass averaged. Temperature determined that way is stored as inlet temperature to the heat exchanger. The mass-average procedure is also used at junctions, thus assuming perfect mixing.

When the displaced volume is higher than the volume of the heat exchanger, the previous approach is inappropriate. In that case, a different method is applied. This can happen when flow rate is high, heat exchanger is small or time step is large. Heat cannot be transferred only to the heat exchanger volume. Therefore, parcels are displaced first and then heat is exchanged with the volume that went through the heat exchanger and is now at the outlet. A new parcel is created as in the standard procedure. This situation did not happen in any of the simulations of the present study. Hence, the first approach was always applied.

Engine cylinders are generally the main contributors to heat rejection. VEMOD includes a lumped heat transfer model of the engine block which takes into account the different heat transfer processes: conduction, convection, radiation, thermal inertia and heat generation [30,38]. Heat transfer coefficient from in-cylinder gas to walls is modeled with a modified Woschni correlation [39,40]. Convective heat transfer from the engine structure to coolant and oil are calculated with correlations of the form of Dittus-Bölter equation [41]. Oil splash is considered by means of a correlation proposed by Bohac et al. [42]. Heat rejection in the turbocharger is also calculated with a lumped thermal network [43]; correlations based on Sieder-Tate equation are used for convective heat transfer both at the air side and at the oil side [44]. All heat transfer submodels are validated and extensively proven.

Case setup

To run the engine simulations, it was necessary to fully define the engine in VEMOD. Information of pump curves, heat exchanger characteristics and thermostat behavior was gathered. Engine geometry was drawn out from the engine CAD. Geometrical data of the external circuits was measured in the test cell. ECU calibration was obtained from the manufacturer.

Circuit layouts were defined as indicated in Figure 3 and Figure 4. Coolant circuit is realistic, but oil circuit is a simplification. Measuring devices are depicted at their locations: thermocouples, flowmeter and pressure transducer. Circuit branches are numbered for internal reference.
It must be noted that, both in the experiment and in the simulations, the engine valve present in branch 3 of the cooling circuit was always wide open. Coolant pump is a turbopump with a pump head curve which is a function of pump speed and flow rate. Oil pump is a positive-displacement pump with a flow rate curve dependent on pump speed and fluid temperature. In both oil and coolant circuits, the oil cooler has a bypass (branch 5 of both circuits). Flow is distributed between oil cooler and bypass. Thus, heat exchange and head loss are limited, and flow is never blocked by fouling of the cooler passages. For the steady-state tests, 5 minutes of engine operation were simulated. This assured that all variables were stable. In the WLTC simulation, the initial conditions of fluids were set to be equal to those of the experimental tests.

All simulations were run in a desktop computer with a quad-core Intel® Core™ i5-6600K processor using four threads. Global calculation time was around 10 times higher than real time.

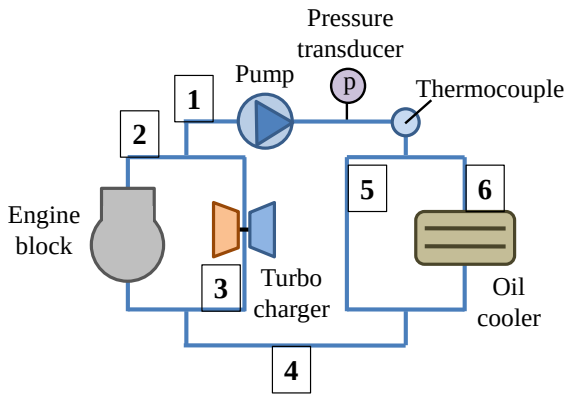

Figure 3. Oil circuit layout.

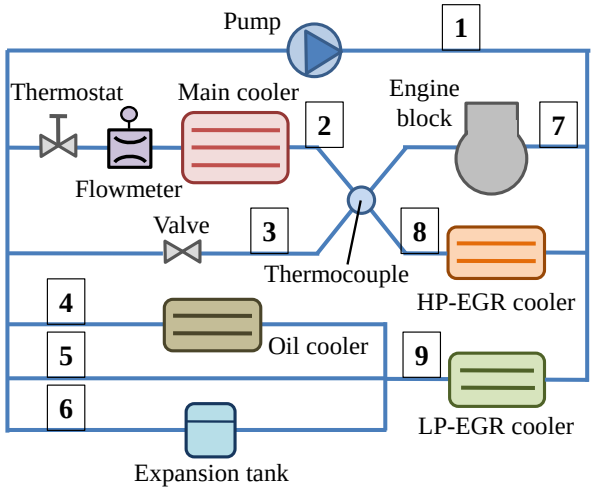

Figure 4. Cooling circuit layout.

Results and discussion

Performance of the thermo-hydraulic model was evaluated with four variables: oil pressure and temperature at pump outlet, coolant flow rate through the cooler and coolant temperature at engine outlet. Measured values of those variables were compared with values obtained from the engine simulation. First, steady-state outcomes are analyzed. Later, results of the WLTC are presented and discussed.

Steady-state

Figure 5 displays the comparison between model and experiment for the variables analyzed in the oil circuit. Two data groups can be identified in the graph on the left (oil pressure). The group with lower pressures comprises operating points with engine speeds of 1000, 1250 and 1500 rpm. Model predictions were in good agreement with measurements. The group with higher pressures was composed by the operating points with engine speeds of 2500 and 3500 rpm. In that group, oil pressure was correctly predicted for tests at 2500 rpm. However, at 3500 rpm measured pressures were higher than simulated pressures. This deficiency was expected to have limited impact on the WLTC simulation because engine speed does not reach 3500 rpm during the cycle. Overall, 83% of the analyzed points had an error lower than 0.5 bar. Mean error was 268 mbar. Oil temperature analysis is shown on the right side of Figure 5. Mean error was 2.15ºC and in 88% of the points error was below 4ºC. Tests done in cold environment were plotted in different color. No systematic errors were observed in model predictions due to those different conditions. In conclusion, performance of the oil circuit model was considered satisfactory.

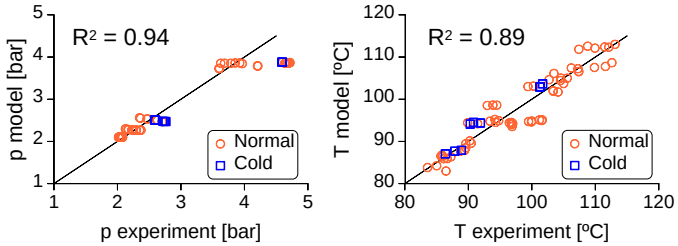

Figure 5. Oil pressure (left) and oil temperature (right) at pump outlet. Steady-state.

Regarding the coolant circuit, flow rate at branch 2 and fluid temperature at engine outlet were analyzed. On the left side of Figure 6, predicted flow rate was plotted against measured flow rate. In general, agreement was good. The largest discrepancies were observed at high engine speeds. Mean error was 5% and 93% of the points presented an error smaller than 10%. Comparison of modeled and experimental coolant temperatures can be seen on the right side of Figure 6. All points were close to the diagonal line except three points corresponding to the three repetitions of the test at 1500 rpm and half load. The highest error was 4ºC, but 91% of the points had an error lower than 2ºC. Mean error was 1.1ºC. Again, no specific limitations were found in model predictions when simulating tests done in cold environment.

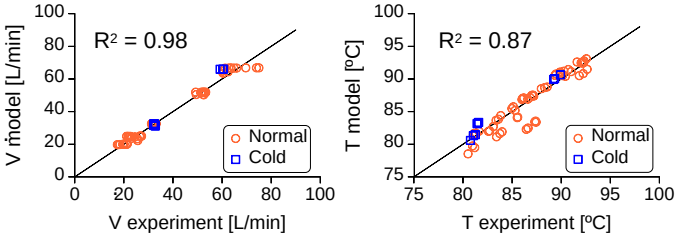

Figure 6. Coolant flow rate through the cooler branch (left) and coolant temperature at engine outlet (right). Steady-state.

Steady-state validation revealed that the thermo-hydraulic model was capable of providing reliable results with acceptable precision. In general, the model was able to capture the influence of engine speed and load in steady operation. Next, model performance in transient conditions was studied.

WLTC

After validation in steady state, the WLTC was simulated. Figure 7 shows the evolution of engine speed and torque during the cycle. The WLTC is a very dynamic cycle with diverse operating conditions. In the upper plot, a comparison between measured and modeled torque can be seen. During most of the cycle, the engine model was capable of reproducing the performance observed in the real engine. Engine speed, on the contrary, was an input to VEMOD. Speed curve during the cycle is shown in the lower plot.

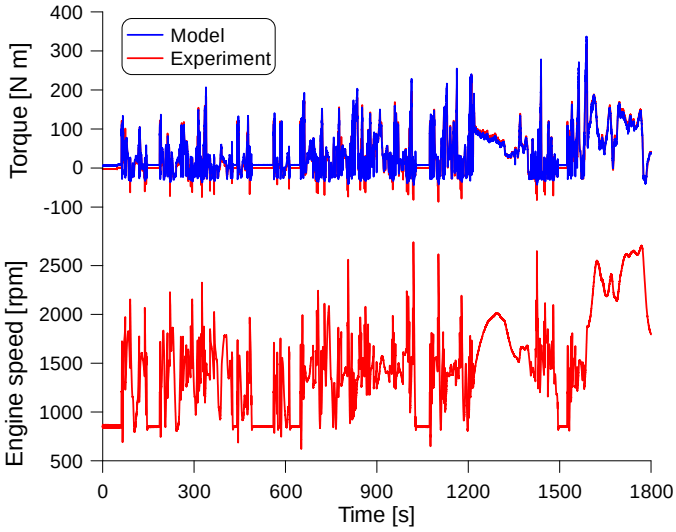

Figure 7. Engine speed and torque. WLTC.

Warmed-up test

In this study, as noted in the *Experimental campaign* section, at the start of the cycle the engine was already warmed up.

In Figure 8, the evolution of oil pressure during the cycle was plotted. Response of oil pump was well predicted by the model. At some peaks, pressure predicted by the model was slightly lower than the measurement. At the end of the cycle, when engine speed was the highest, oil pressure was slightly overpredicted, as in the steady-state tests at high engine speed. Overall, only small discrepancies were observed, even though the circuit simplification. This further encouraged confidence in the validity of the simplified circuit to emulate the behavior of the real circuit.

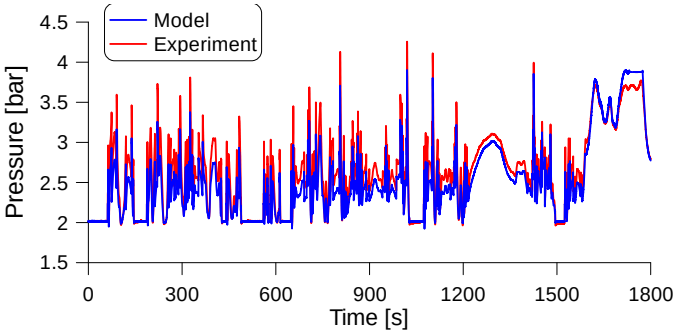

Figure 8. Oil pressure at pump outlet. Warmed-up WLTC.

Oil temperature was examined next. Comparison between model and experiment is shown in Figure 9. The model captured the measured trend during the first half of the cycle and at the last part. In other parts, temperature was underpredicted up to 4.7ºC. Thermal inertia was right at some instants but at others the model was too fast. Mean error was 1.4ºC. During 92% of the time, error was below 3ºC. Most of the time, modeled temperatures were below experimental temperatures. Specifically, 94% of the error was due to underprediction.

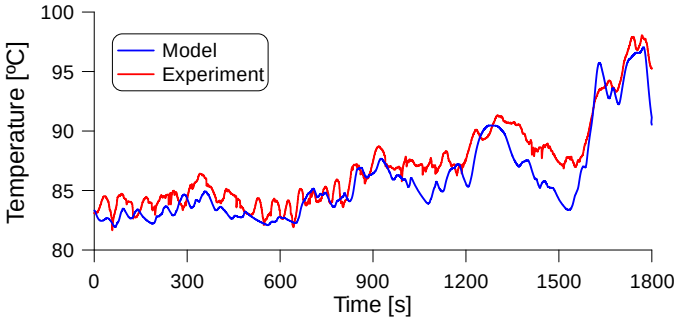

Figure 9. Oil temperature at pump outlet. Warmed-up WLTC.

Coolant flow rate presented the trends displayed in Figure 10. There was a clear underestimation of the coolant flow rate through the cooler at high engine speed. This decreases cooling and therefore produces increased coolant temperature in the simulation. However, coolant temperature was not determined solely by the flow in the cooler branch: cooler has a bypass (branch 3) and the cooling circuit has a branch that does not go through the engine (branch 9), as can be seen in
Figure 4. Therefore, the final effect on coolant temperature was limited. Opening degree of the thermostat, according to the model, is indicated by the dashed line. Modeled flow rate follows the opening trace. When the thermostat opens for the first time, opening degree reaches 33.6%. During the rest of the cycle, it varies between 1% and 17%.

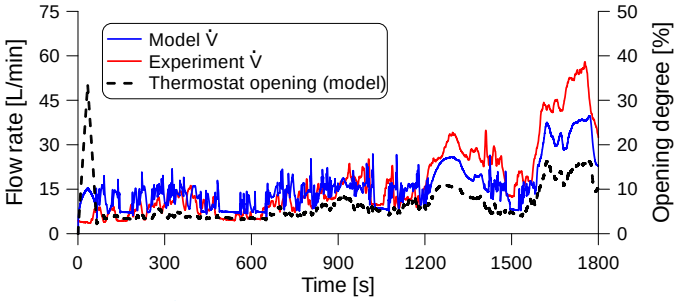

Figure 10. Coolant flow rate through the cooler branch. Warmed-up WLTC.

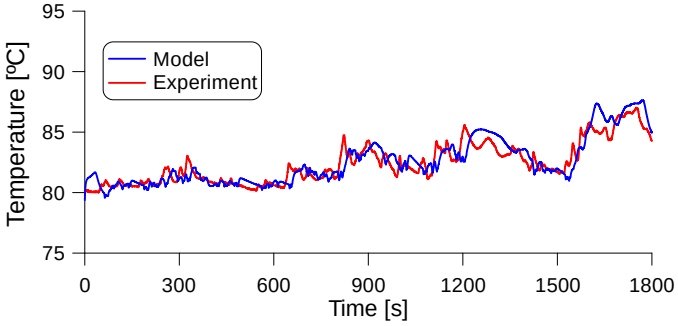

Figure 11. Coolant temperature at engine outlet. Warmed-up WLTC.

In Figure 11, modeled coolant temperature is plotted against the measured curve. As expected, temperature was higher than the reference at the instants when flow rate though the cooler was lower than the measured value. Nevertheless, the maximum error was 3ºC. Circuit configuration provided robustness to the prediction. As discussed, there were several parallel coolant paths, thus deviations in one of them were not critical. Overall, trends of coolant temperature were well captured. Mean error was 0.7ºC. For 90% of the cycle, error was below 1.5ºC. The modeled curve was above the experimental curve 56% of the time, which comprised 60% of the

error. Consequently, there was a slight tendency to overestimation. In general, thermal inertia was slightly larger than in the experiment. The small inaccuracies in thermal inertia both in the oil and the coolant circuits can be attributed to uncertainties in the volume of the network.

Test starting from ambient temperature

In this study, engine and fluids start the WLTC at the ambient temperature of 20ºC.

First, the evolution of measured and simulated oil pressures was analyzed. In the warmed-up test, it was observed that simulated pressure could be lower than measured pressure at some peaks, but the difference was small (see Figure 8). In the present test, there was a clearer disagreement during the first quarter of the cycle, as can be seen in Figure 12. A likely cause of this is due to the effect of temperature on oil viscosity, because the misprediction happened when oil temperature was below 60ºC. At lower temperatures, oil viscosity is higher, which in turn increases friction in tubes and, hence, head losses. This points out a suitable improvement of the model: calculating the friction coefficient as a function of flow conditions instead of using a constant value. Once oil was warm, prediction was better. Its accuracy was then comparable with the one of the warmed-up test.

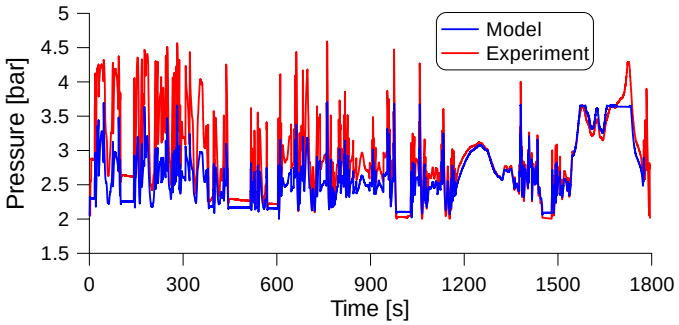

Figure 12. Oil pressure at pump outlet. WLTC with warm-up.

A comparison between measured and simulated oil temperature can be seen in Figure 13. During most of warm-up, the agreement was very good. For 84% of the cycle duration, error was below 4ºC. Mean error was 2.1ºC. Thermal inertia was well captured by the model. However, the experiment shows an initial delay of oil warm-up which was not reproduced by the model. Moreover, during the second half of the cycle, prediction deteriorates slightly. The maximum error of the cycle was 5.2 ºC.

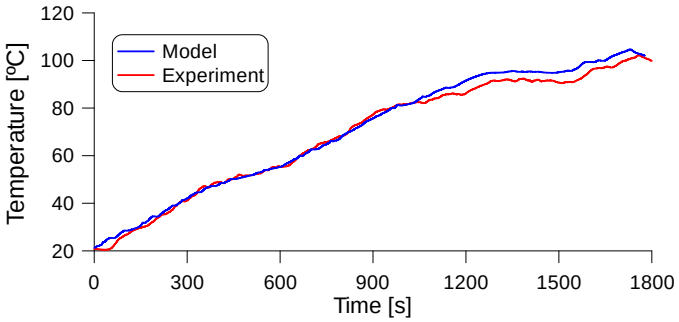

Figure 13. Oil temperature at pump outlet. WLTC with warm-up.

Next, coolant flow rate was examined. In the upper part of Figure 14, measured and modeled flow rates are plotted. In the lower part, opening degree of the thermostat calculated by the model is given. According to the model, the thermostat began to open between 1000 s and 1100 s. This was consistent with the change of trend observed in coolant temperature in that interval, as seen in Figure 15. The flowmeter was unable to measure any flow quantity before 1600 s, though. This was due to the measuring range of the flowmeter, whose lower limit was 4.5 L/min. Opening degree of the thermostat was very low (around 1%) during this test. In addition, the thermostat was continuously opening and closing. This resulted in very low flow rates through the cooler. Under these circumstances, uncertainty was high. In spite of that, it can be mentioned that predicted flow rate through the coolant cooler was in the same order of magnitude of the measured values.

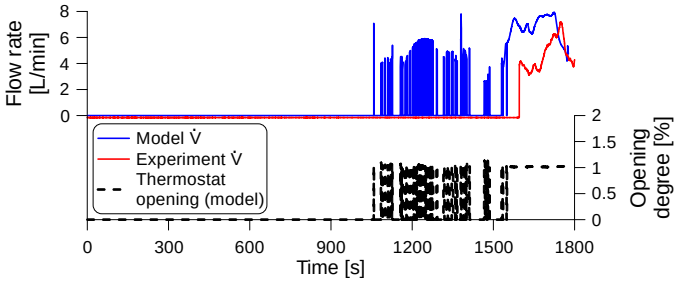

Figure 14. Coolant flow rate through the cooler branch. WLTC with warm-up.

Finally, the prediction of coolant temperature during the WLTC was assessed. In Figure 15, the experimental and the modeled curve are plotted together. A very good agreement between model and experiment was obtained. Mean error was 1.6ºC. During 87% of the time, error was below 3ºC. Thermal inertia was well captured. Moreover, the model was able to correctly predict the slope change at 600 s. As in oil temperature, the measured curve shows an initial delay of warm-up which was not reproduced by the simulation. This causes a maximum error of 5.3ºC.

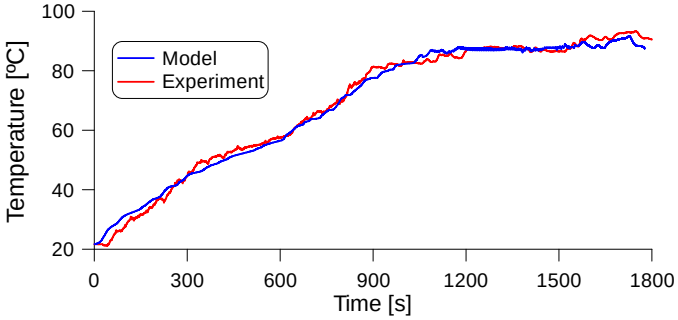

Figure 15. Coolant temperature at engine outlet. WLTC with warm-up.

Summary/Conclusions

This paper presented the validation of a thermo-hydraulic model integrated in a global engine model. The model solves both the hydraulic network and the thermal evolution in a hydraulic circuit. Model workflow and characteristics were thoroughly explained. Interactions with other submodels of the global engine model were described. To accomplish the validation goals, an extensive experimental campaign was conducted with a production diesel engine. Steady-state tests consisted of 22 operating points to evaluate model performance at different engine speeds and loads both in usual (20ºC) and in cold (-7ºC) environment. Additionally, the WLTP driving cycle was measured under two conditions: with the engine already warmed up and starting the engine at ambient temperature. The WLTC was suitable to test the model under highly dynamic,

transient operation. The thermo-hydraulic model was capable of providing reliable results with acceptable precision if engine definition and boundary conditions were accurate. Still, some discrepancies at high engine speeds or low oil temperatures were detected. Nonetheless, they had limited impact on the prediction of coolant and oil temperatures, which was the primary goal of the work. In the transient tests, thermal response was satisfactorily modeled. Mean errors of coolant and oil temperatures were between 0.7ºC and 2.1ºC. Upcoming work will cover the validation of the thermo-hydraulic model in driving cycles under cold ambient conditions. Model improvements to overcome the limitations observed during this work are of particular interest as well. Eventually, the aim of the Virtual Engine Model is to study engine performance and emissions in various scenarios.

References

1. Martin, J., Arnau, F.J., Piqueras, P. and Auñón, A., "Development of an integrated Virtual Engine Model to simulate new standard testing cycles," SAE Technical Paper 2018-01-1413, 2018
2. Torregrosa, A., Olmeda, P., Garcia-Ricos, A., Natividad, J. and Romero, C.A., "A Methodology for the Design of Engine Cooling Systems in Standalone Applications," SAE Technical Paper 2010-01-0325, 2010, doi:10.4271/2010-01-0325
3. Gao, Z., Conklin, J.C., Daw, C.S. and Chakravarthy, V.K., "A proposed methodology for estimating transient engine-out temperature and emissions from steady-state maps," *International Journal of Engine Research*, 11, 2, 137 – 151, 2010, doi:10.1243/14680874JER05609
4. Xin, J., Shih S., Itano E., Maeda, Y. et al., "Theoretical Consideration to Improve Engine Cooling and Application of Coupling 3D Combustion Simulations with Heat Transfer in Water Jacket and Components," *Honda R&D technical review*, 15, 2, 117-125, 2003, NII:40005956609
5. Choi, KW., Kim, KB. and Lee, KH., "Investigation of emission characteristics affected by new cooling system in a diesel engine," *J Mech Sci Technol*, 23, 7, 1866-1870, 2009, doi:10.1007/s12206-009-0616-9
6. Pang, H., Brace, C. and Akehurst, S., "Potential of a Controllable Engine Cooling System to Reduce NOx Emissions in Diesel Engines," SAE Technical Paper 2004-01-0054, 2004, doi:10.4271/2004-01-0054
7. Gumus, M., "Reducing cold-start emission from internal combustion engines by means of thermal energy storage system," *Applied Thermal Engineering*, 29, 4, 652-660, 2009, doi:10.1016/j.applthermaleng.2008.03.044
8. Allen, D. and Lasecki, M., "Thermal Management Evolution and Controlled Coolant Flow," SAE Technical Paper 2001-01-1732, 2001, doi:10.4271/2001-01-1732
9. Trapy, J. and Damiral, P., "An Investigation of Lubricating System Warm-up for the Improvement of Cold Start Efficiency and Emissions of S.I. Automotive Engines," SAE Technical Paper 902089, 1990, doi:10.4271/902089
10. Cortona, E. and Onder, C., "Engine Thermal Management with Electric Cooling Pump," SAE Technical Paper 2000-01-0965, 2000, doi:10.4271/2000-01-0965
11. Broatch, A., Luján, J. M., Ruiz, S. and Olmeda P., "Measurement of hydrocarbon and carbon monoxide emissions during the starting of automotive DI diesel engines," *International Journal of Automotive Technology*, 9, 2, 129−140, 2008, doi:10.1007/s12239−008−0017−6
12. Romero, C., Torregrosa, A., Olmeda, P., and Martin, J., "Energy Balance During the Warm-Up of a Diesel Engine," SAE Technical Paper 2014-01-0676, 2014, doi:10.4271/2014-01-0676
13. Roberts, A., Brooks, R. and Shipway, P., "Internal combustion engine cold-start efficiency: A review of the problem, causes and potential solutions," *Energy Conversion and Management*, 82, 327-350, 2014, doi:10.1016/j.enconman.2014.03.002
14. Osman, A., Muhammad Yusof, M. and Rafi, M., "Vehicle Testing and Development Involving a Simplified Split Cooling with Integrated Exhaust Heat Recovery and Reuse," SAE Technical Paper 2016-01-0647, 2016, doi:10.4271/2016-01-0647
15. Goettler, H., Vidger, L. and Majkrzak, D., "The effect of exhaust-to-coolant heat transfer on warm-up time and fuel consumption of two automobile engines," SAE Technical Paper 860363, 1986, doi:10.4271/860363
16. Taylor, O., Pearson, R. and Stone, R., "Reduction of CO2 Emissions through Lubricant Thermal Management During the Warm Up of Passenger Car Engines," SAE Technical Paper 2016-01-0892, 2016, doi:10.4271/2016-01-0892
17. Luptowski, B., Arici, O., Johnson, J. and Parker, G., "Development of the Enhanced Vehicle and Engine Cooling System Simulation and Application to Active Cooling Control," SAE Technical Paper 2005-01-0697, 2005, doi:10.4271/2005-01-0697
18. Cipollone, R. and Villante, C., "A Fully Transient Model For Advanced Engine Thermal Management," SAE Technical Paper 2005-01-2059, 2005, doi:10.4271/2005-01-2059
19. Cipollone, R., Di Battista, D. and Gualtieri, A., "A novel engine cooling system with two circuits operating at different temperatures," *Energy Conversion and Management*, 75, 581-592, 2013, doi:10.1016/j.enconman.2013.07.010.
20. Torregrosa, A.J., Broatch, A., Olmeda, P. and Romero C., "Assessment of the influence of different cooling system configurations on engine warm-up, emissions and fuel consumption," *International Journal of Automotive Technology*, 9, 4, 447−458, 2008, doi:10.1007/s12239−008−0054−1
21. Caresana, F., Bilancia, M. and Bartolini, C.M., "Numerical method for assessing the potential of smart engine thermal management: Application to a medium-upper segment passenger car," *Applied Thermal Engineering*, 31, 16, 2011, 3559-3568, 2011, doi:10.1016/j.applthermaleng.2011.07.017
22. Park, K.S., Won, J.P. and Heo, H.S., "Thermal flow analysis of vehicle engine cooling system," *KSME International Journal*, 16, 7, 975-985, 2002, doi:10.1007/BF02949727
23. Banjac, T., Wurzenberger, J.C. and Katrašnik, T., "Assessment of engine thermal management through advanced system engineering modeling," *Advances in Engineering Software*, 71, 19-33, 2014, doi:10.1016/j.advengsoft.2014.01.016
24. Regulation (EC) No 715/2007 of the European Parliament and of the Council of 20 June 2007 on type approval of motor vehicles with respect to emissions from light passenger and commercial vehicles (Euro 5 and Euro 6) and on access to vehicle repair and maintenance information, Official Journal of the European Union, June 2007.
25. Galindo, J., Serrano, J.R., Arnau, F.J. and Piqueras, P., "Description of a Semi-Independent Time Discretization Methodology for a One-Dimensional Gas Dynamics Model," *Journal of Engineering for Gas Turbines and Power*, 131, 034504-5, 2009, doi:10.1115/1.2983015
26. Galindo, J., Tiseira, A., Navarro, R., Tarí, D., et al., "Compressor efficiency extrapolation for 0D-1D engine simulations," SAE Technical Paper 2016-01-0554, 2016, doi:10.4271/2016-01-0554
27. Serrano, J.R., Arnau, F.J., García-Cuevas, L.M., Dombrovsy, A. and Tartoussi, H., "Development and validation of a radial

turbine efficiency and mass flow model at design and off-design conditions," *Energy Conversion and Management*, 125, 281-293, 2016, doi:10.1016/j.enconman.2016.09.032
28. Payri, F., Olmeda, P., Martín, J., García, A., "A complete 0D thermodynamic predictive model for direct injection diesel engines," *Applied Energy*, 88 (12) 4632–4641, 2011, doi:10.1016/j.apenergy.2011.06.005
29. Arrègle, J., López, J., Martín, J. and Mocholí, E., "Development of a Mixing and Combustion Zero-Dimensional Model for Diesel Engines," SAE Technical Paper 2006-01-1382, 2006, doi:10.4271/2006-01-1382
30. Torregrosa, A.J., Olmeda, P., Martín, J. and Romero, C., "A tool for predicting the thermal performance of a Diesel engine," *Heat transfer engineering* 32 (10) (2011) 891-904, doi:10.1080/01457632.2011.548639
31. Payri, F., Olmeda, P., Martín, J. and Carreño, R., "A new tool to perform global energy balances in DI Diesel engines," *SAE Int. J. Engines* 7(1):43-59, 2014, doi:10.4271/2014-01-0665
32. Payri, F., Arnau, F.J., Piqueras, P. and Ruiz, M.J., "Lumped Flow-Through and Wall-Flow Monolithic Reactors Modelling for Real-Time Automotive Applications," SAE Technical Paper 2018-01-0954, 2018
33. Martín, J., Piqueras, P., García-Cuevas, L.M. and Sanchis, E.J., "Lumped DOC modelling approach for fluid-dynamic simulation under engine dynamic operation", presented at 15th EAEC European Automotive Congress, 2017
34. Shah, R.K. and Sekulic, D.P., "Fundamentals of Heat Exchanger Design," *John Wiley & Sons* (2003), ISBN: 978-0-471-32171-2.
35. Boulos P.F., Lansey, K.E. and Karney, B.W., "Comprehensive Water Distribution Systems Analysis Handbook for Engineers and Planners, Second Edition," *MWH Soft*, 2006, ISBN: 9780974568959.
36. Eigen, eigen.tuxfamily.org, accessed Sept. 2017.
37. Powell, M. J. D., "An efficient method for finding the minimum of a function of several variables without calculating derivatives," *Computer Journal*, **7** (2): 155–162, 1964, doi:10.1093/comjnl/7.2.155
38. Torregrosa, A.J., Olmeda, P., Degraeuwe, B. and Reyes, M., "A concise wall temperature model for DI Diesel engines," *Applied Thermal Engineering*, 26 (11–12), 1320-1327, 2006, doi:10.1016/j.applthermaleng.2005.10.021
39. Payri, F., Margot, X., Gil, A. and Martin, J., "Computational Study of Heat Transfer to the Walls of a DI Diesel Engine," SAE Technical Paper 2005-01-0210, 2005, doi:10.4271/2005-01-0210
40. Broatch, A., Olmeda, P., García, A., Salvador-Iborra, J. and Warey, A., "Impact of swirl on in-cylinder heat transfer in a light-duty diesel engine," *Energy*, 119, 1010-1023, 2017, doi:10.1016/j.energy.2016.11.040
41. Dittus, F.W. and Boelter, L.M.K., "Heat transfer in automobile radiators of the tubular type," *International Communications in Heat and Mass Transfer*, 12, 1, 3-22, 1985, doi:10.1016/0735-1933(85)90003-X
42. Bohac, S., Baker, D. and Assanis, D., "A Global Model for Steady State and Transient S.I. Engine Heat Transfer Studies," SAE Technical Paper 960073, 1996, doi:10.4271/960073
43. Payri, F., Olmeda, P., Arnau, F.J., Dombrovsky, A. and Smith, L., "External heat losses in small turbochargers: Model and experiments," *Energy*, 71, 534-546, 2014, doi:10.1016/j.energy.2014.04.096
44. Serrano, J.R., Olmeda, P., Arnau, F.J., Reyes-Belmonte, M.A. and Tartoussi H., "A study on the internal convection in small turbochargers. Proposal of heat transfer convective coefficients," *Applied Thermal Engineering*, 89, 587-599, 2015, doi:10.1016/j.applthermaleng.2015.06.053

Contact Information

Dr. Pablo César Olmeda
CMT-Motores Térmicos, Universitat Politècnica de València
Camí de Vera s/n, 46022 Valencia (Spain)
Phone: +34 963877650
pabolgon@mot.upv.es

Acknowledgments

This research has been partially funded by the European Union's Horizon 2020 Framework Programme for research, technological development and demonstration under grant agreement 723976 ("DiePeR") and by the Spanish government under the grant agreement TRA2017-89894-R. Josep Salvador-Iborra was supported by Universitat Politècnica de València through the contract FPI-S2-2016-1357 of the program PAID-01-16. The authors wish to thank Renault SAS, especially P. Mallet and E. Gaïffas, for supporting this research. Jaime Monfort San Segundo is acknowledged for his helpful collaboration in the code implementation.

Definitions/Abbreviations

CAD	crank angle degree
C_p	specific heat capacity
g	gravity acceleration
HP-EGR	high pressure exhaust gas recirculation
LP-EGR	low pressure exhaust gas recirculation
m	mass
p	pressure
T	fluid temperature
$\dot{V}$	flow rate
ρ	density